arTs Università degli Studi di Trieste
Archivio della ricerca – postprint

A new soluble and bioactive polymorph of praziquantel

Debora Zanolla[a], Beatrice Perissutti[a,*], Nadia Passerini[b], Michele R. Chierotti[c], Dritan Hasa[d], Dario Voinovich[a], Lara Gigli[e], Nicola Demitri[e], Silvano Geremia[a], Jennifer Keiser[f], Paolo Cerreia Vioglio[g], Beatrice Albertini[b]

[a] *Department of Chemical and Pharmaceutical Sciences, University of Trieste, P.le Europa 1/via L. Giorgieri 1, 34127 Trieste, Italy*
[b] *Department of Pharmacy and BioTechnology, University of Bologna, Via S. Donato 19/2, 40127 Bologna, Italy*
[c] *Department of Chemistry and NIS Centre, University of Torino, V. Giuria 7, 10125 Torino, Italy*
[d] *Leicester School of Pharmacy, De Montfort University, The Gateway, LE1 9BH Leicester, United Kingdom*
[e] *Elettra – Sincrotrone Trieste, S.S. 14 Km 163.5 in Area Science Park, 34149 Basovizza, Trieste, Italy*
[f] *Helminth Drug Development Unit, Department of Medical Parasitology and Infection Biology, Swiss Tropical and Public Health Institute, Socinstr. 57, CH-4051 Basel, Switzerland*
[g] *Aix-Marseille Université, CNRS, ICR (UMR 7273), 13397 Marseille cedex 20, France*

ARTICLE INFO

Keywords:
Praziquantel
Mechanochemistry
Solid-state reactions
Polymorphism
Solubility
Bioactivity
Crystal structure solution
DFT-D calculations
Neglected tropical diseases

ABSTRACT

Praziquantel is the only available drug to treat Schistosomiasis. However, its utilization is limited by many drawbacks, including the high therapeutic dose needed, resulting in large tablets and capsules difficult to be swallowed, especially from pediatric patients. In this study, an alternative option to overcome these disadvantages is proposed: to switch to a novel crystalline polymorph of racemic compound praziquantel. The preparation of the crystalline polymorph was realized via a neat grinding process in a vibrational mill. The new phase (Form B) was chemically identical to the starting material (as proved by HPLC, ^{1}H NMR, and polarimetry), but showed different physical properties (as evaluated by SEM, differential scanning calorimetry, thermogravimetry, ATR-FTIR spectroscopy, X-ray powder diffraction, and solid-state NMR). Furthermore, the crystal structure of the new phase was solved from the powder synchrotron X-ray diffraction pattern, resulting in a monoclinic *C2/c* cell and validated by DFT-D calculation. Moreover the simulated solid-state NMR ^{13}C chemical shifts were in excellent agreement with the experimental data. The conversion of original praziquantel into Form B showed to affect positively the water solubility and the intrinsic dissolution rate of praziquantel. Both the in vitro and in vivo activity against *Schistosoma mansoni* were maintained. Our findings suggest that the new phase, that proved to be physically stable for at least one year, is a promising product for designing a new praziquantel formulation.

1. Introduction

Praziquantel (PZQ) is an antihelmintic drug largely used for the treatment of Schistosomiasis. It is estimated that at least 230 million people worldwide are infected by the genus Schistosoma [1], mainly with *Schistosoma haematobium*, *S. japonicum* and *S. mansoni*. Praziquantel is included in the WHO Model List of Essential Drug for the treatment of adults and children [2]. The drug is well tolerated and safe, however it is classified as a BCS class II drug, hence characterized by high permeability, low solubility [3] and extensive first-pass metabolism [4]. The recommended dosage for the treatment of schistosomiasis is 20 mg/kg three times a day which has to be repeated after 4 to –6 weeks. For at-risk populations a 40 mg/kg single dose is used as preventive chemotherapy. Since children are the main target of treatment, research is needed to enhance the solubility and the bioavailability of PZQ, in order to reduce the high therapeutic doses and therefore the dimension of tablets, which are difficult to swallow particularly for pediatric patients [5]. Several studies aimed to enhance PZQ properties such as the preparation of solid dispersion of the drug with Povidone [6–8] , or with Sodium Starch Glycolate [9], Praziquantel-Beta-Cyclodextrins systems [10,11], solid lipid nanoparticles [12], coground systems [13], fast dispersible granules [14] and melt

Abbreviations: ASU, Asymmetric Unit; ATR-FTIR, Attenuated Total Reflectance Fourier Transform Infrared Spectroscopy; CPMAS, Cross Polarization Magic Angle Spinning; DFT-D, Dispersion-corrected Density Functional Theory; DSC, Differential Scanning Calorimetry; HPLC-UV, High Performance Liquid Chromatography Ultraviolet Detection; IC50, Half Maximal Inhibitory Concentration; IDR, Intrinsic Dissolution Rate; NMR, Nuclear Magnetic Resonance; PZQ, Starting Praziquantel; SD, Standard Deviation; RSD, Relative Standard Deviation; SEM, Scanning Electron Microscopy; SSNMR, Solid State Nuclear Magnetic Resonance; TGA, Thermogravimetric Analysis; XRPD, X-Ray Powder Diffraction

* Corresponding author.
E-mail address: bperissutti@units.it (B. Perissutti).

Accepted 29 January 2018

granulation combined with ultrasonic spray congealing [15].

In this study, an alternative way to improve solubility and hence to possibly reduce the therapeutic dose is proposed, namely to switch to a crystalline polymorph of PZQ racemic compound.

Polymorphism, a property inherent to the solid state, is the ability of a compound to exist in more than one crystalline form that have different arrangements in the solid state. Polymorphs have different relative intermolecular and/or interatomic distances, or unit cells. Sometimes structural differences are significant, resulting in very different physical (e.g. mechanical, thermal, etc.) and chemical properties (e.g. chemical reactivity). In other cases differences are very subtle making it difficult to distinguish different crystal forms [16–18]. The search for these polymorphic varieties recently became a topic of major interest.

Several authors have already testified the existence of crystal modifications of PZQ. The commercial racemic compound crystallizes in an anhydrous crystal form. Its structure (TELCEU in CSD) belongs to the triclinic space group P-1 with four crystallographically independent molecules in the asymmetric unit with a *syn* conformation (concerning the two C = O groups present in the molecules), where two of them are disordered [19].

Differently from the racemic PZQ, the pure enantiomers (R) or (S)-PZQ crystallize in hemihydrates having different intermolecular interactions than those of the racemic crystal [20,21]. Racemic praziquantel is well known also as an excellent candidate to form co-crystals with several aliphatic dicarboxylic acids, such as oxalic, malonic, succinic, maleic, fumaric, glutaric, adipic, and pimelic acid [19].

Recently, the formation of a diastereoisomeric cocrystal pair with L-malic acid in presence of acetone and the subsequent isolation of R-enantiomer has been also documented [22].

As regards to anhydrous polymorphic varieties of racemic praziquantel, previous works have tried to obtain new polymorphs of racemic PZQ, by slow evaporation using several solvents, but always they obtained the same triclinic crystal form [23].

By exploiting the full potential of a multitechnique approach here we report a detailed investigation of a new polymorphic anhydrous crystalline form of PZQ (Form B) obtained by a neat grinding method in absence of solvent. The identification of the polymorph was carried out by differential scanning calorimetry, thermogravimetry, SEM analysis, solid-state NMR (SSNMR) combined with DFT-D calculations, ATR-FTIR. The crystalline structure was solved from the powder X-ray diffraction pattern and deposited in the Cambridge Crystallographic Data Center with deposition number: 1,557,658. The new phase have been also fully characterized for its biopharmaceutical properties (determining saturation solubility and intrinsic dissolution rate), and performing in vitro and in vivo antihelmintic assays.

2. Materials and methods

2.1. Materials

Praziquantel (PZQ) Ph. Eur. grade ((11bRS)-2-(Cyclohexylcarbonyl)-1,2,3,6,7,11b-hexahydro-4-H-pyrazino[2,1-a]isoquinolin-4-one) was kindly donated by Fatro S.p.A. (Bologna, Italy). PZQ impurity A (2-Benzoyl-1,2,3,6,7,11b-hexahydro-4-H-pyrazino[2,1-a]isoquinolin-4-one) and impurity B (2-Cyclohexanecarbonyl-2,3,6,7-tetrahydro-pyrazino[2,1-a]isoquinolin-4-one) were Ph. Eur. grade and purchased from Endotherm Gmbh (Saarbruecken, Germany). HiPersolv Chromanorm Methanol (Ph. Eur. for HPLC Gradient Grade) and Ethanol (Ph. Eur.) were purchased from VWR Chemicals BHD PROLABO®.

2.1.1. Preparation of Form B

Praziquantel was milled on its own, by neat grinding, in a vibrational mill-Retsch MM400 (Retsch GmbH) which was equipped by 2 screw-type zirconium oxide jars, each with a capacity of 35 ml. A ceramic material like zirconium oxide was selected due to its high density (5.9 g/cm^3), allowing for a high energy input. The amount of powder to be introduced in the milling jar was determined in 0.800 g per jar, and three zirconium oxide spheres of 15 mm (weighing 10.72 g) were used as milling media. The vibrational frequency of 20 Hz was applied for a time of 4 h without interruption.

After the treatment, the solid product were stored at 25 °C in desiccators over anhydrous calcium chloride.

2.2. Methods

In all evaluations the ground sample was analyzed in comparison to starting PZQ racemic compound.

2.2.1. Determination of drug content

Reverse phase HPLC-UV method was used for the quantification of PZQ, using a method adapted from literature [24] and validated according to a slight modification in column length. The HPLC system used consisted of two mobile phase delivery pumps (LC-10 ADVP, Shimadzu, Japan), a UV–Vis detector (SPD-10Avp, Shimadzu, Japan), an autosampler (SIL-20A, Shimadzu, Japan), an interface (SCL-10Avp, Simadzu, Japan) for the acquisition of data through a software Ez-Star and a column Kinetex 5 μm C18 100 Å (150 × 4.60 mm, Phenomenex, Bologna, Italy). The mobile phase comprised of methanol and water (65:35 V/V), the flow rate was 1 ml/min and absorbance readings were conducted at fixed wavelength of 220 nm. The retention time of PZQ was about 5.5 min and the run time was set at 12 min. Quantification was carried out by integration of the peak areas using the external standardization method. Under these conditions, the linear calibration curve of PZQ was obtained in the range of 0.3–10 mg/l (r^2 = 0.99996). As reference, a fresh stock solution was prepared each time before starting the analysis. The standard solution of Praziquantel was prepared by dissolving 10 mg of PZQ in 20 ml of methanol HPLC-grade. The solution was stirred for several minutes and then diluted with the mobile phase in ratios 1:10 and 1:20 to obtain a drug concentration of 2.5 mg/l (ppm). According to the PZQ monograph in the Eur. Ph. (Ed. 8.0), specified impurities, named impurity A and impurity B, have to be detected. The linear calibration curve of each impurity was obtained in the range of 0.05–1 mg/l (r^2 = 0.9993 and 0.9994, for impurity A and B, respectively). The retention times of the impurities were at 3.45 min and 11.2 min. Both impurities were absent in the reference solution. The same procedure was used to characterize starting PZQ solid form and the milled sample Form B.

The determination of the PZQ content into the milled samples was determined by dissolving about 10 mg, exactly weighed, of sample in 20 ml of methanol HPLC-grade. The obtained solution was then diluted 1:200 with the mobile phase, corresponding to about 2.5 mg/l of PZQ, in order to ensure the linearity of the analytical response. In the sample solution, the retention time of PZQ was at about 5.4–5.5 min. Each sample solution was analyzed in triplicate and the mean of the sum of the peak responses of Praziquantel was then calculated. The results were expressed as the percentage of PZQ recovery with respect to the sum of all peaks present in the chromatogram (PZQ and eventual related impurities and/or other detectable related products).

2.2.2. Polarimetric analyses

Optical rotations of the samples were measured on a Polarimeter Jasco P-2000 (Lecco, Italy), with a λ = 589 nm and a concentration of 1 g/100 ml in ethanol, according to the method reported in literature [25,26]. Ethanol was preferred in place of $CHCl_3$, in order to prevent formation of air bubbles in the cell.

2.2.3. X-Ray powder diffraction (XRPD)

Starting PZQ material was tested on a conventional diffractometer equipped with an RTMS X'celerator detector, using a Ni-filtered Cu Kα radiation (wavelength 1.5418 Å). A small amount of powder (15–25 mg) was gently pressed on a glass slide to give a flat surface. The

data were collected in the 2θ range 3–40° at room temperature.

2.2.4. Synchrotron X-Ray powder diffraction

A diffraction pattern with improved resolution and signal to noise ratio of Form B was collected at the X-ray diffraction beamline (XRD1) of the Elettra Synchrotron, Trieste (Italy) [27]. Powder diffraction pattern was collected in transmission mode, at room temperature (25 °C) with a monochromatic wavelength of 0.700 Å (17.71 KeV) and 200·200 μm^2 spot size, using a Dectris Pilatus 2 M hybrid-pixel area detector.

Form B powder has been packed in borosilicate capillaries with a 300 μm diameter (10 μm wall thickness).

The bidimensional powder pattern have been integrated using Fit2D program [28], after preliminary calibration of hardware setup, using a capillary filled with LaB_6 standard reference powder (NIST 660a).

2.2.5. Thermal analyses

Differential Scanning Calorimetry analysis were carried out with a DSC Mettler-Toledo DSC822e (Greifensee, Switzerland) connected to a cell Mettler DSC20 calorimeter, equipped with the STARe software. Two mg of both samples, were placed in aluminum perforated crucibles with a capacity of 25 μL, heated at a scanning rate of 10 °C/min in a temperature range between 30 and 180 °C, under a nitrogen atmosphere. The calibration of the instrument was performed with indium, zinc and lead for the temperature, and with indium for the measurement of the enthalpy.

Thermogravimetric analyses were performed on a Mettler-Toledo TGA/SDTA851e instrument. Samples of approximately 10 mg were placed in 40 μL aluminum pans and heated from 30 to 220 °C with a heating rate of 10 °C/min, under nitrogen atmosphere. Resulting weight–temperature diagrams were analyzed using STARe software 11.00 to calculate the weight loss.

2.2.6. Solid-state NMR measurements

Solid-state NMR measurements were performed on a Bruker Avance II 400 instrument operating at 400.23, 100.65 and 40.55 MHz for ^{1}H, ^{13}C and ^{15}N nuclei, respectively. Cylindrical 4 mm o.d. zirconia rotors with a sample volume of 80 μL were employed and spun at 12 (^{13}C) and 9 (^{15}N) kHz. All experiments employed the RAMP-CP pulse sequence (^{1}H 90° pulse = 3.05 μs) with the TPPM ^{1}H decoupling with an rf field of 75 kHz during the acquisition period. 124 transients were acquired with 3.5 ms of contact time and relaxation delays of 20 and 30 s for PZQ and Form B, respectively. ^{13}C and ^{15}N chemical shifts were referenced with the resonance of hexamethylbenzene (^{13}C methyl signal at 17.4 ppm) and $(NH_4)_2SO_4$ (^{15}N signal at -355.8 ppm with respect to CH_3NO_2).

2.2.7. DFT calculations

Periodic lattice calculations were performed by means of CASTEP [29] Academic Release version 17.2 which exploits a plane-wave and pseudopotential approach within density functional theory (DFT) [30]. Magnetic shieldings were calculated using the GIPAW algorithm [31] as implemented in the CASTEP code. The geometry optimization and the NMR chemical shift calculations were carried out employing the generalized gradient approximation (GGA) PBE exchange-correlation functional [32] with the semi-empirical dispersion scheme [33] TS [34] and ultrasoft pseudopotentials which were generated on the fly. The crystal structure of the polymorph determined from PXRD data was used as the starting structure for the geometry optimization. The plane-wave cut-off energy was set equal to 700 eV. The Brillouin zone was automatically sampled using a Monkhorst-Pack grid with a *k*-point spacing of 0.05 $Å^{-1}$. The geometry optimization was performed with the unit cell parameters fixed, as they were considered to be of acceptable quality from the experimental data. The refined structure was used in the subsequent magnetic shielding calculation, using the same cut-off energy as above. The theoretical absolute ^{13}C and ^{15}N isotropic magnetic shielding (σ_{iso}) values were converted into the corresponding isotropic chemical shifts (δ_{iso}) relative to the absolute magnetic shielding of the reference substance glycine computed at the same level. The following conversion was used: $\delta_{iso} = \sigma_{ref} - \sigma_{iso}$, where σ_{ref} is the reference shielding of glycine, here 170.1 ppm for ^{13}C and 192.9 ppm for ^{15}N.

2.2.8. ATR-FTIR spectroscopy

ATR-FTIR spectra of both commercial PZQ and Form B were performed at the solid state without any dilution using a spectrophotometer Perkin Elmer Spectrum 100 FT-IR (Beaconsfield, England), equipped software PE version 6.3.4. copyright 2008, attached to a Universal ATR sampling accessory. The range analyzed ranged from 650 cm^{-1} to 4000 cm^{-1}, with scan number equal to 4.

2.2.9. Scanning electron Microscopy (SEM)

Samples were metallized with S150A Sputter Coater (Edwards High Vacuum, Crawley, West Sussex, UK) and then observed under a scanning electron microscope Leica Stereoscan 430i (Leica Cambridge Ltd., Cambridge, UK).

2.2.10. Determination of drug solubility

Solubility measurements of both starting PZQ and Form B were carried by adding an excess amount of the drug to 10 ml of deionized water, respectively. The suspensions were agitated in the dark, at 20 °C for 48 h, to ensure that equilibrium was attained, and then filtered through a membrane (pore size 0.2 μm). Finally, 1 ml of each solution, previously diluted 1:200 with the mobile phase, was assayed by HPLC analysis, following the previously described method. Each sample was analysed in triplicate and the average was reported. Forty-eight hours was found to be enough to reach the equilibrium, whilst an agitation time of 72 h or superior in aqueous medium showed a pronounced chemical degradation of the drug according to the results previously published by Suleiman and coworkers [35].

2.2.11. Intrinsic dissolution studies

The intrinsic dissolution rate (IDR) of commercial PZQ and Form B, was determined from powder tablets obtained with a hydraulic press (PerkinElmer, Norwalk, USA). Sample tablets of 150 mg were directly compressed at a pressure of 1 tons for 60 s in a stainless steel cylinder that served as sample holder. The tablets resulted of a diameter of 1 cm and with a flat surface area of 0.785 cm^2. The sample holders were placed in 1000 ml of distilled water at 37 °C and stirred at a rotation speed of 100 rpm (the distance between paddle and tablet surface was 3.5 cm). At predetermined time points (10–20–30–40–50–60 min), 2 ml of aliquots were withdrawn and immediately replaced with 2 ml of dissolution medium. The obtained samples were then analyzed by HPLC-UV (as previously described). All dissolution experiments were conducted at least in triplicate and both the SD (%) and the RSD (%) were calculated at each time point. The slopes of the intrinsic dissolution curves (amount of drug dissolved per unit area over time) were compared by applying linear regression.

The dissolution behavior of the samples was compared by performing a Student's *t*-test and the curves were considered statistically different with p values $< .05$.

2.2.12. Determination of in vitro and in vivo activity against adult Schistosoma mansoni

In vitro and in vivo studies were carried out in accordance with Swiss national and cantonal regulations on animal welfare (permission no. 2070) at the Swiss Tropical and Public Health Institute (Basel, Switzerland) as described earlier [36]. Female mice (NMRI strain; weight ~ 20–22 g) were purchased from Charles River, Germany, kept under environmentally-controlled conditions (temperature ~ 25 °C; humidity ~ 70%; 12-hour light and 12-hour dark cycle) with free access to water and rodent diet and acclimatized for one week before

infection. Cercariae of *Schistosoma mansoni* were obtained from infected intermediate host snails (*Biomphalaria glabrata*).

For the in vitro studies adult Schistosomes obtained via dissection from infected mice were incubated in the presence of the test compounds at different concentrations (0.021–0.33 μg/ml) for up to 72 h. Phenotypes were monitored at several time points based on motility, viability and morphological alterations under an inverse microscope (Carl Zeiss, Germany, magnification 80×). Parasite viability values of treated and untreated worms obtained from microscopic evaluation were averaged (means +/− standard deviation) using Microsoft Excel software. IC_{50} values were calculated using CompuSyn software.

For the in vivo studies groups of 4 infected NMRI mice characterized by a patent *S. mansoni* infection (49 days postinfection) were treated orally with the test drugs via single oral doses (400 mg/kg). Untreated mice (n = 9) served as controls.

Three weeks post-treatment, animals were sacrificed by the CO_2 method and dissected. Worms were sexed and counted [37].

Worm burdens of treated mice were compared to those of control animals, and reductions of worm burden were calculated.

2.2.13. Physical stability during storage

In order to check possible modifications of solid state within time XRPD analyses of ground samples were repeated for a period of 12 months. During storage time, the solid samples were stored in desiccators over anhydrous calcium chloride at room temperature.

3. Results and discussion

The solvent-free mechanical treatment, here presented, was used to obtain a new polymorph from the commercial racemic anhydrous Praziquantel phase. In particular, PZQ was milled on its own via neat grinding, at the operating conditions mentioned in the experimental section, selected after preliminary trials. The yield of the process was almost complete, no relevant phenomena of adhesion nor mechanochromism were noticed. The new polymorphic variety (Form B) was subjected to extensive characterizations, starting from ^{1}H NMR spectrometry, HPLC analysis and polarimetric analysis to check possible chemical modification after grinding. Recorded ^{1}H NMR Spectra (data not shown for brevity), corresponded to data reported in the literature [25] and confirmed the presence of two rotamers of praziquantel, attesting the lack of chemical changes in PZQ after mechanochemical treatment. HPLC results showed a very little amount of impurities formed during the mechanical treatment (0.42%) and a final drug recovery of 99.58% (mean values, n = 3). Nevertheless the amount of impurities is never exceeding USP/EP acceptance criteria.

Due to the fact that PZQ is a racemic compound [38–40], the samples were also evaluated for optical rotation to quantify the enantiomeric excess. Both the samples have a $[\alpha]_\lambda$ (mean ± SD, n = 3) approaching zero. In particular a value of 0.5 ± 2.9 and 0.1 ± 1.6 were registered, for starting PZQ and Form B, respectively, corresponding to a calculated enantiomeric excess of 0.4 and 0.1, as expected for a racemic compound. In agreement with the literature data for conventional racemic compound [9], the SEM images reported in Fig. 1 show the acicular shape of the crystals of the starting PZQ, similar to matchwoods, with diameter of about 60–100 μm and a thickness of 10–15 μm. SEM analysis revealed that Form B has a very different habit and size, and the powder appeared to be formed by agglomerates of long and very thin whiskers (Fig. 2).

The X-ray powder diffraction pattern (Fig. 3) of the starting Praziquantel recorded at room temperature, shows sharp Bragg peaks, confirming the remarkable crystallinity of the sample. The peak positions are in agreement with the diffraction pattern of the racemic form, whose structure has been determined by Espinosa-Lara and coworkers [19] as belonging to the triclinic space group *P*-1 with four crystallographically independent molecules with syn conformation in the asymmetric unit, of which two are disordered. The same authors identified 3 homodimeric motifs in this crystal structure, of which two consist of two and four C−H···O contacts, respectively (motifs III and IV), while described the remaining (motif VII) as a homodimeric C−H···π complex.

The diffraction pattern of the polymorphic variety obtained via neat grinding is presented in Fig. 4. The comparison with the diffraction pattern of raw PZQ (Fig. 3) clearly indicates that the two crystalline phases are different.

The diffraction pattern of the polymorphic variety obtained via neat grinding is presented in Fig. 4. The comparison with the diffraction pattern of raw PZQ (Fig. 3) clearly indicates that the two crystalline phases are different. Due to the sample peaks broadening, the correct indexing of the powder pattern was very challenging. Several solutions were found using the program EXPO2014 [41]. Notwithstanding one solution led to a meaningful model and it belongs to a monoclinic unit cell with a volume of 3369.97 Å^3, very similar to the volume of raw PZQ. The space group suggested is the centrosymmetric *C*2/*c*. Assuming a reasonable density for a fully organic molecular crystal, the number of formula units per unit cell could be determined as Z = 8. A first whole powder pattern fitting (Pawley method) on the experimental powder pattern resulted in a good Rwp of 1.52%. The refined unit cell parameters obtained are a = 21.991(1) Å, b = 5.8884(3) Å, c = 27.331(1) Å, α = 90°, β = 107.787(5)° and γ = 90° with a calculated density of 1.232 g·cm^{-3}. The whole spectrum is well reproduced both at low and high angles of 2θ, with the exception of two peaks at 7.01 and 10.2° of 2θ, having modest intensity, attributable to a minor solid phase not yet identified.

To solve the structure a simulated annealing approach as implemented in TOPAS V5 [42] have been applied successfully, starting from a molecular model obtained from SIGBUG structure [43] after the removal of the water molecule. The solution showing the best agreement with experimental data is shown in Fig. 5. This solution bear one molecule in the asymmetric unit (ASU) in agreement with SSNMR characterization. The Rietveld refinement of the Form B structure yielded an R-Bragg factor of 1.96% (Fig. 4).

The Form B model proposed shows limited steric violations and a meaningful density (Packing Index calculated with PLATON VOID routine [44] is 66.6% for Form B, close to the Packing Index of 67% found for the starting PZQ racemic phase).

Fig. 1. SEM images of starting racemic PZQ (Magnification 500 X (left), 1.00 K X (middle), 5.00 K X (right).

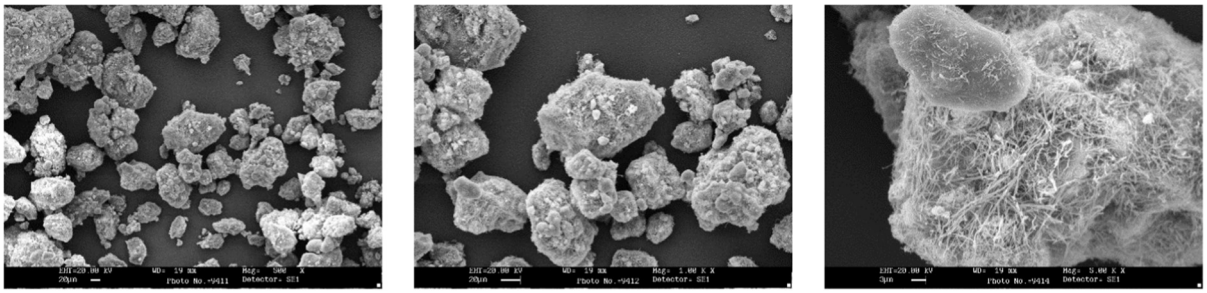

Fig. 2. SEM images of the polymorphic variety B (Magnification 500 X (left), 1.00 K X (middle), 5.00 K X (right).

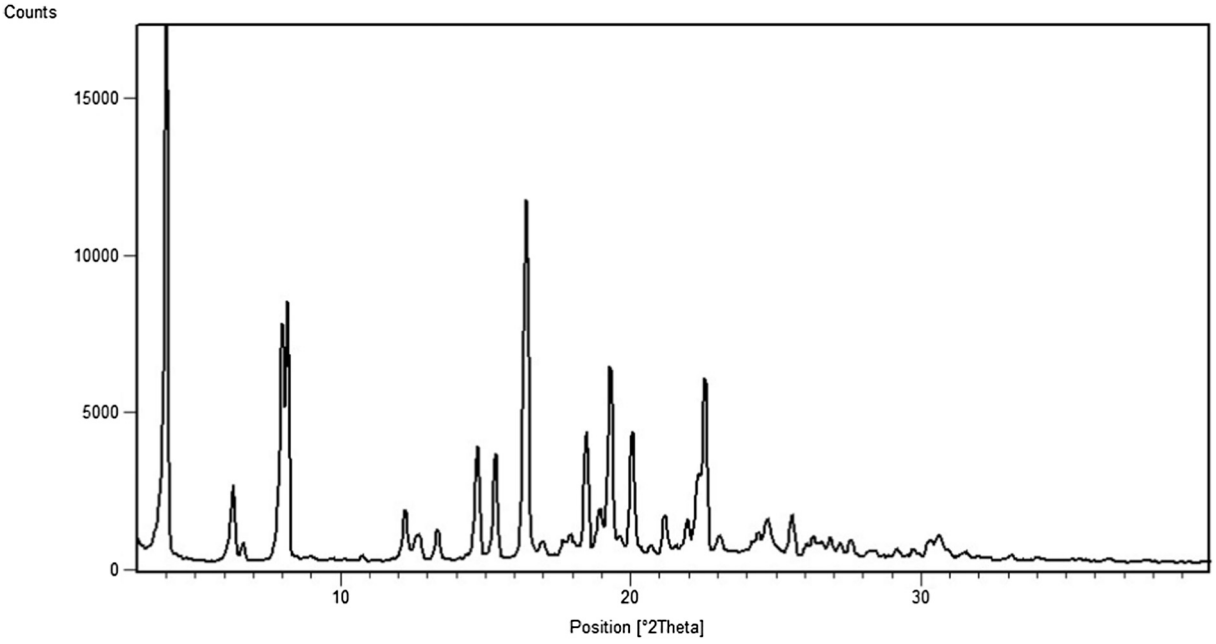

Fig. 3. Powder X-ray diffraction pattern of raw PZQ (recorded using a Ni-filtered Cu Kα radiation, wavelength: 1.5418 Å).

To highlight the differences between the polymorphs, the crystal packing are shown in Fig. 6.

The ^{13}C and ^{15}N CPMAS spectra, reported in Figs. 7 and 8, respectively confirm and highlight the difference between the two phases. In fact, it is well known that different crystal packing significantly change the position of the peaks in the SSNMR spectra owing to the new chemical and magnetic environment experienced by the atoms [45–47].

All chemical shifts with assignment are listed in Table 1. For atom numbers we refer to Scheme 1.

The ^{13}C CPMAS spectrum of starting PZQ is characterized by the splitting of all signals, particularly clear for the resonance around 164 ppm assigned to the carbonyl C4, giving rise to several sets of signals (with different intensity). This indicates the presence of four crystallographically independent molecules in the unit cell in agreement with the X-ray structure. The ^{13}C CPMAS spectrum of Form B is completely different from initial crystal PZQ indicating the formation of a new phase. Indeed, the spectrum is characterized by a single set of resonances in agreement one independent molecule in the unit cell (see above) instead of four. The peaks are very sharp (FWHM ~ 100 Hz) indicating the formation of a highly crystalline compound, all shifted of about 0.2–3 ppm compared to original PZQ. The same conclusions can be drawn from the ^{15}N CPMAS spectra (Fig. 8) where sharper and slightly shifted signals are observed for Form B with respect to PZQ. No peaks due to raw PZQ are observed in both ^{13}C and ^{15}N CPMAS spectra of Form B indicating the quantitative conversion during the mechanochemical process.

The structural model obtained from synchrotron X-ray powder data was further optimized by solid-state DFT-D calculations using the fixed lattice with unit-cell parameters from Rietveld refinement and with atomic positions fully relaxed. The optimization confirmed the centrosymmetric *C2/c* space group, and the optimized model was very close to that one obtained by Rietveld refinement (Fig. S2 in Supplementary Information). To verify the reliability of the optimization, the chemical shifts were computed by the GIPAW method and compared with the experimental ones (Table 1). Experimental and computed ^{13}C isotropic chemical shift values show an excellent agreement. The Root-Mean-Square Deviation (RMSD) is 2.4 ppm. Based on the literature and on our own experience [48,49], an RMSD value of about 2.2 ± 0.5 ppm is expected for a correct model.

In the ATR-FTIR spectrum of starting PZQ (Fig. 9, bottom), according to literature data [9,15,21,40,50] the following main peaks were detected: in the range 3000–2900 cm^{-1} (stretching vibrations of $–CH_2$ and –CH), 1650–1720-cm^{-1} (stretching of carbonyl groups and bending of CH bonds of the aromatic rings), in the 1500–1400 cm^{-1} (vibrations of stretching of aromatic C and bending vibrations of $–CH_2$), and at around 760 cm^{-1} (bending vibration of aromatic-CH). In the spectra of Form B (Fig. 9, top) there are significant differences in terms of position and transmittance. Worth of notice the modification in the doublet at 1700–1600 cm^{-1} that is well resolved in starting PZQ, whilst the two peaks nearly overlapped in polymorphic variety B. In particular, as visible in the frame, starting PZQ shows two signals at 1647 and 1624 cm^{-1} attributable, in accordance to Borrego-Sanchez et al. [50], to the symmetric stretching mode of the heterocyclic carbonyl and to that of the carbonyl group joined to the cyclohexyl,

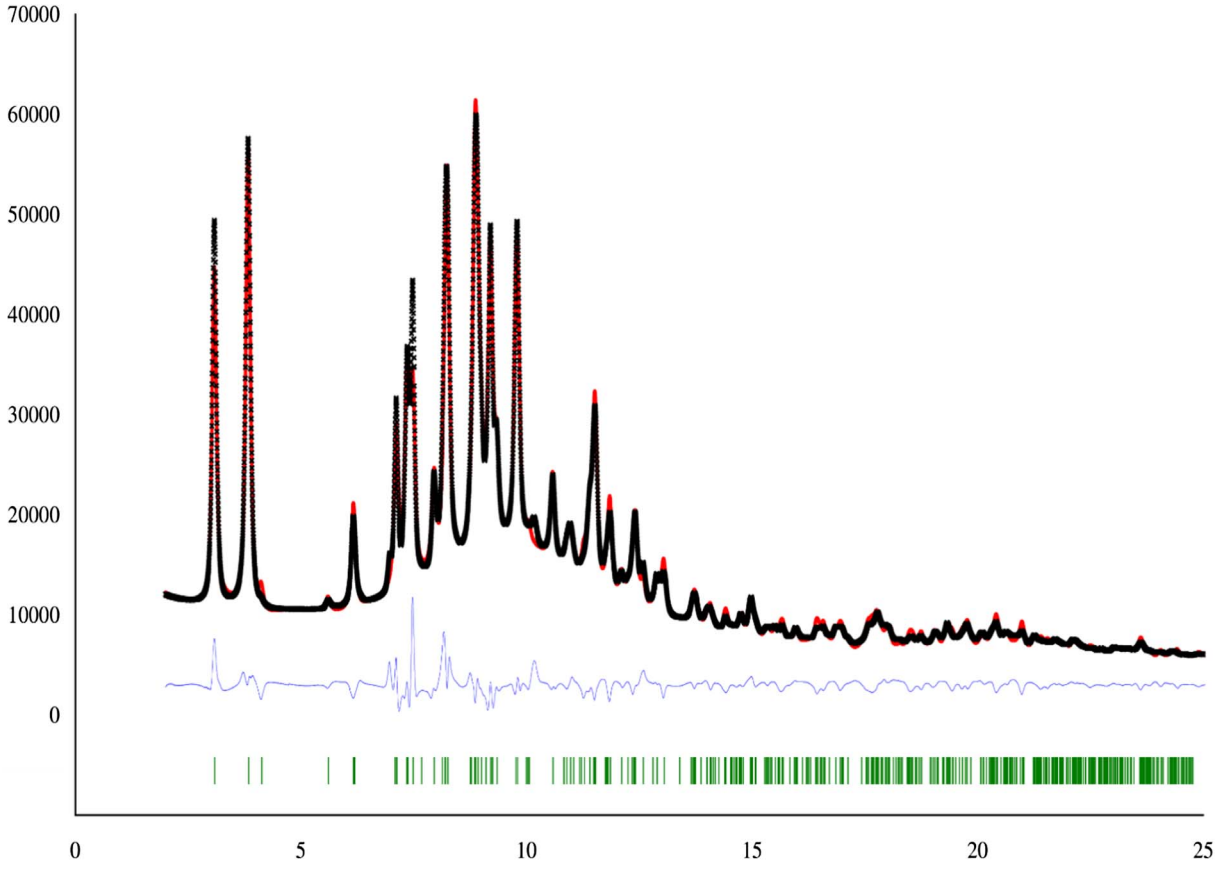

Fig. 4. Rietveld refinement profile fit (obtained after the simulating annealing calculated with TOPAS V5) of PZQ Form B: in black the experimental pattern (recorded using synchrotron radiation, wavelength: 0.700 Å), in red the calculated one. The residual are displayed on the bottom in blue and the reflection ticks in green. For interpretation of the references to color in this figure legend, the reader is referred to the web version of this article.

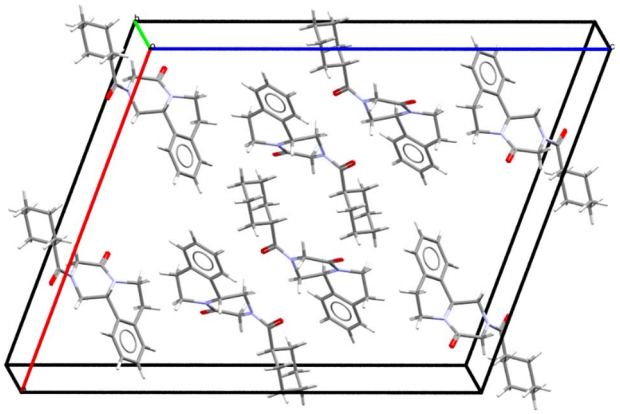

Fig. 5. Capped stick representation of the proposed structure for Form B. The monoclinic unit cell found hosts 8 molecules, one crystallographically independent, assuming a *C*2/*c* space group.

respectively.

Further, a typical shoulder appears at the high frequency slope of the experimental band (ranging about 1668 cm^{-1}), as indicated by an arrow in Fig. 9.

In polymorphic variety B, in accordance to Borrego-Sanchez et al. [21] the frequency difference in ν(CO) between both carbonyl groups is lower, due to the presence of the conformers *anti* (as visible in Fig. 5) instead of *syn* (contrariwise present in the original PZQ). Hence the different positions detected in ATR-FTIR spectra of the two signals assigned to the stretching of CO groups are a further confirmation of a different crystal packing.

These results were also confirmed by comparing FTIR spectra of both samples acquired with high resolution (reported for brevity in supplementary information, Fig. S3).

The thermal behavior of ground sample was analyzed by DSC and TGA. In the TGA analyses (data not shown) the anhydrous nature of both Form B and PZQ was assessed. The DSC curves recorded in nitrogen atmosphere (Fig. 10) revealed that the ground sample is characterized by an endothermic peak at 112.10 °C, attributed to its melting event, with a melting enthalpy of 56.57 J/g. Also, no dehydration event was observed, confirming its anhydrous nature.

When compared with the starting PZQ, with a melting point of 142.56 °C in agreement with the reported data [39], the ground sample shows a decrease of about 30 °C. It should be noted that, in the light of the previous characterization data, this low temperature melting cannot be associated with the melting of a very small crystals of native phase [51], via a Gibbs-Thompson effect. Thus melting point difference reinforces, among others characterization results, the differences in the nature of the crystals and consequently, in the lattice energy of these phases.

To evaluate the suitability of this polymorphic variety for the purpose of the research, that is improving PZQ solubility, and hence possibly reduce the therapeutic dose, water solubility and intrinsic dissolution rate were determined.

The new phase, as reported in Table 2, has double water solubility in comparison to PZQ (equilibration time = 48 h). This data strengthen the idea that the new crystalline phase has a different free energy compared to original PZQ.

To check biopharmaceutical performances and to exclude the effects of experimental variables (such as particle size, stirring pattern, etc.) intrinsic dissolution rate (IDR) of both original PZQ and Form B was

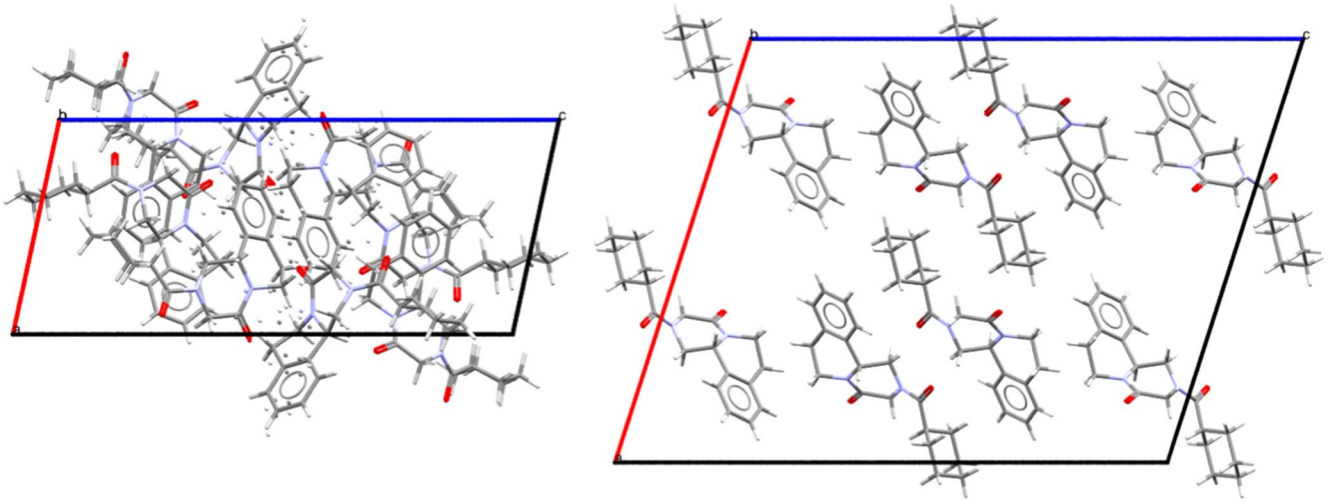

Fig. 6. Crystal packing of PZQ (left) and Form B (right) viewed along b axis. Complete packing view is reported in Supplementary Information (Fig. S1).

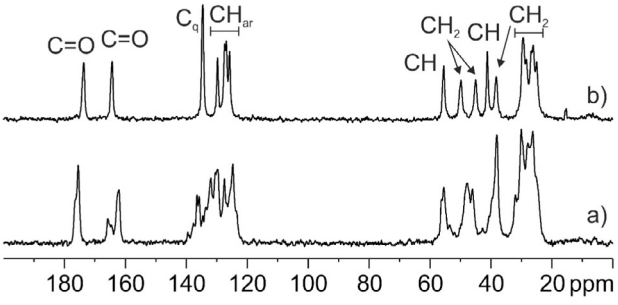

Fig. 7. ^{13}C (100.65 MHz) CPMAS spectra with principal group assignments of PZQ (a) and Form B (b) recorded at 12 kHz.

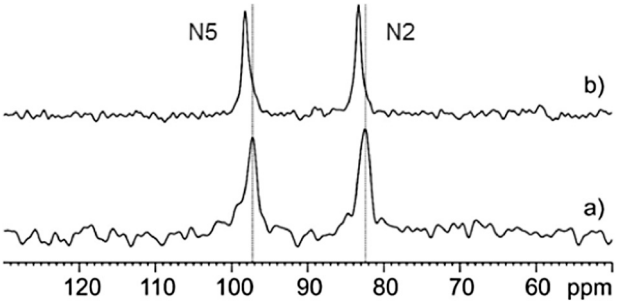

Fig. 8. ^{15}N (40.55 MHz) CPMAS spectra with assignments of PZQ (a) and Form B (b) recorded at 9 kHz.

determined. This is a standardized kinetic method defined as the dissolution rate of pure substances, after compaction, in constant surface conditions.

As shown in Table 2 and Fig. 11, the intrinsic dissolution rate (IDR) of the polymorphic variety, higher of a factor of 2 than PZQ resulted significantly different from that of pure PZQ (Student's *t* test: $p < .0004$).

The in vitro antischistosomal activity of commercial PZQ and polymorphic variety against adult *S. mansoni* was determined. The IC_{50} values of Form B demonstrated that was highly active against *S. mansoni* (IC_{50} = 0.135 μg/ml compared to 0.165 μg/ml of starting PZQ), proving the in vitro activity remained unaffected after neat grinding.

In a pilot study, the polymorphic variety was then orally administered to a group of 4 infected mice characterized by a patent *S. mansoni* infection, in a single dose of 400 mg/kg. Forty nine days post infection a worm burden reduction of 100% was obtained in mice treated with the

Table 1
Experimental and computed ^{13}C and ^{15}N chemical shifts (ppm) with assignments for PZQ and Form B.

Atom	Group	PZQ exp	Form B exp	Form B calc
		^{13}C		
7′	C=O	175.4, 176.2 sh	173.6	172.6
4	C=O	165.8, 164.6, 162.1	164.3	163.3
7a	C_q	137.7, 136.5	134.6	135.7
11a	C_q	135.8, 134.6	134.6	136.4
8	CH	129.7, 127.5, 124.8	129.8	130.5
11	CH	133.7, 132.0, 130.5	127.5	128.2
10	CH		126.9	127.0
9	CH		125.8	126.1
11b	CH	56.3, 55.5	55.5	54.6
3	CH_2	46.1	49.8	47.8
1	CH_2	47.9	45.0	41.6
1′	CH	39.7	41.2	38.5
6	CH_2	38.1	38.3	35.1
6′	CH_2	32.0, 30.1, 27.9, 26.3, 25.3	29.4	26.1
2′	CH_2		29.4	26.4
7	CH_2		28.4	25.0
4′	CH_2		26.7	24.0
3′	CH_2		26.1	22.4
5′	CH_2		25.0	21.6
		^{15}N		
5	N	97.2	98.2	101.8
2	N	82.4	83.3	86.7

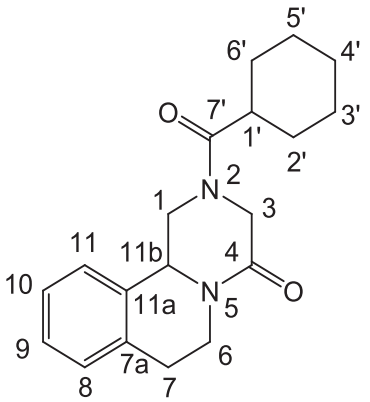

Scheme 1. Chemical structure of PZQ with atom numbering.

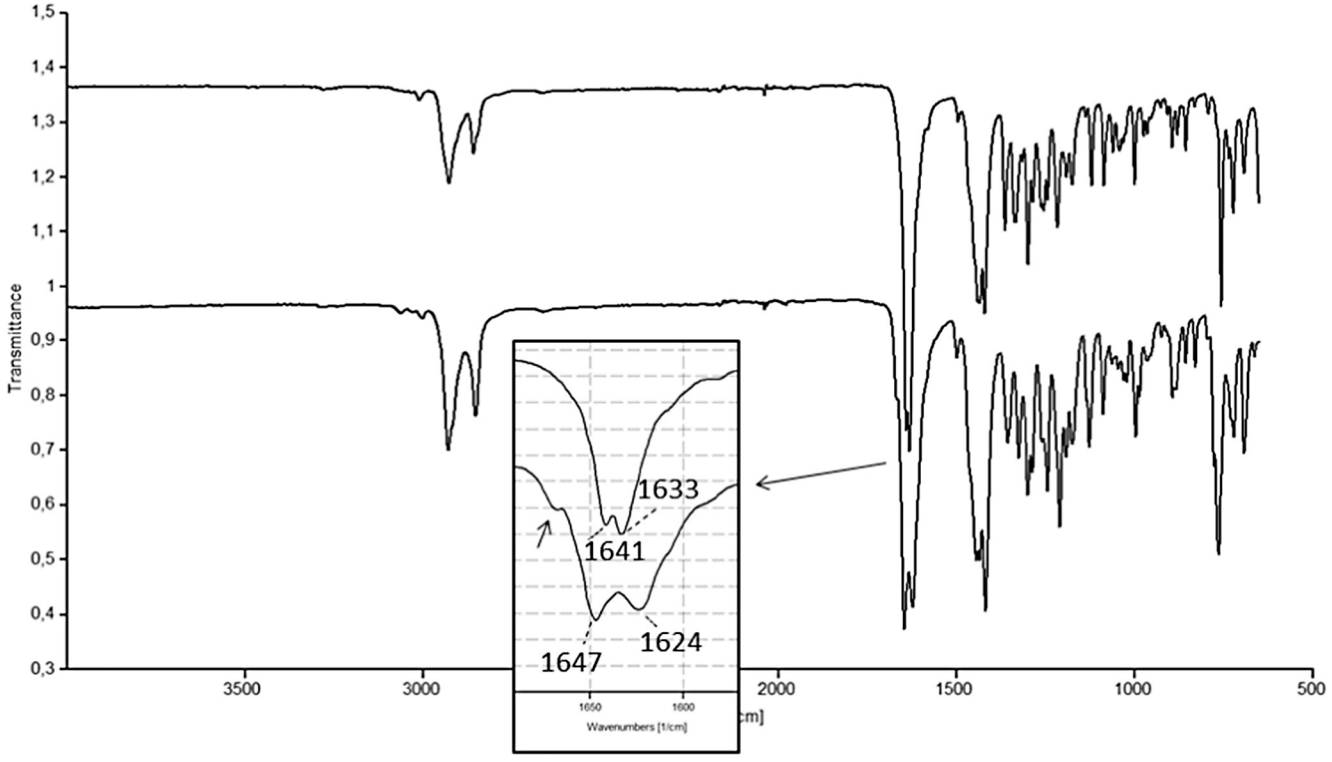

Fig. 9. ATR-FTIR spectra of starting PZQ (bottom) compared to Form B (top); an enlarged image of the 1700–1600 cm^{-1} spectrum range is available in the frame.

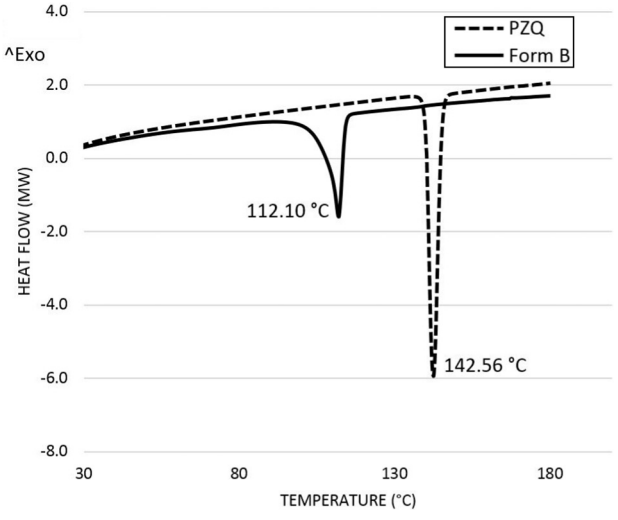

Fig. 10. DSC traces of original PZQ and polymorphic variety B.

Table 2
Solubility (Cs) and intrinsic dissolution rate in water (mean ± S.D., n = 3).

Sample	Cs at 20 °C mg/l	IDR at 37 °C µg*cm^{-2} min^{-1}
PZQ	140.30 ± 9.26	31.2 ± 0.6
Form B	281.31 ± 8.32	62.2 ± 1.3

polymorphic variety B, compared to about 98% of starting PZQ.

Finally, the stability study revealed that the polymorphic phase B was physically stable under dry conditions at room temperature for at least 12 months as indicated by the XRPD diffractogram identical to that of the fresh sample (as reported in Fig. S4).

4. Conclusions

A new polymorphic variety of racemic Praziquantel is here presented. The polymorphic form B was obtained from the original racemic compound via a simple solvent-free process: a neat grinding in vibrational mill. The new polymorph was fully characterized and the crystal structure, corresponding to a monoclinic *C*2/*c* cell, was solved from the powder X-ray diffraction pattern. The structure has been confirmed by periodic DFT calculations. Excellent agreement is observed between experimental and calculated ^{13}C data in solid-state NMR spectra. Interestingly, the new phase exhibited favourable biopharmaceutical properties: high in vitro and in vivo bioactivity against *S. mansoni* and prolonged physical stability. Further studies of in vivo efficacy of this phase are necessary to determine its minimum therapeutic dose. However, from the above reported experimental evidence, the new polymorphic variety is a very promising product for the treatment of Schistosomiasis, and for designing a new praziquantel formulation for treating children.

Acknowledgements

The authors gratefully thank Dr. Teresa Gianferrara, Dr. Samuel Golob for their help in the data analysis and for the constructive discussions. M.R.C. is indebted with Jeol Company for helpful technical assistance and cooperation. P.C.V. thanks Dr. Giulia Mollica for helpful discussion.

Conflict of interest

The authors declare no conflict of interest.

Funding Sources

This work was supported by University of Trieste – Finanziamento di Ateneo per Progetti di Ricerca Scientifica – FRA 2015. This work was granted access to the HPC resources of Aix-Marseille Université

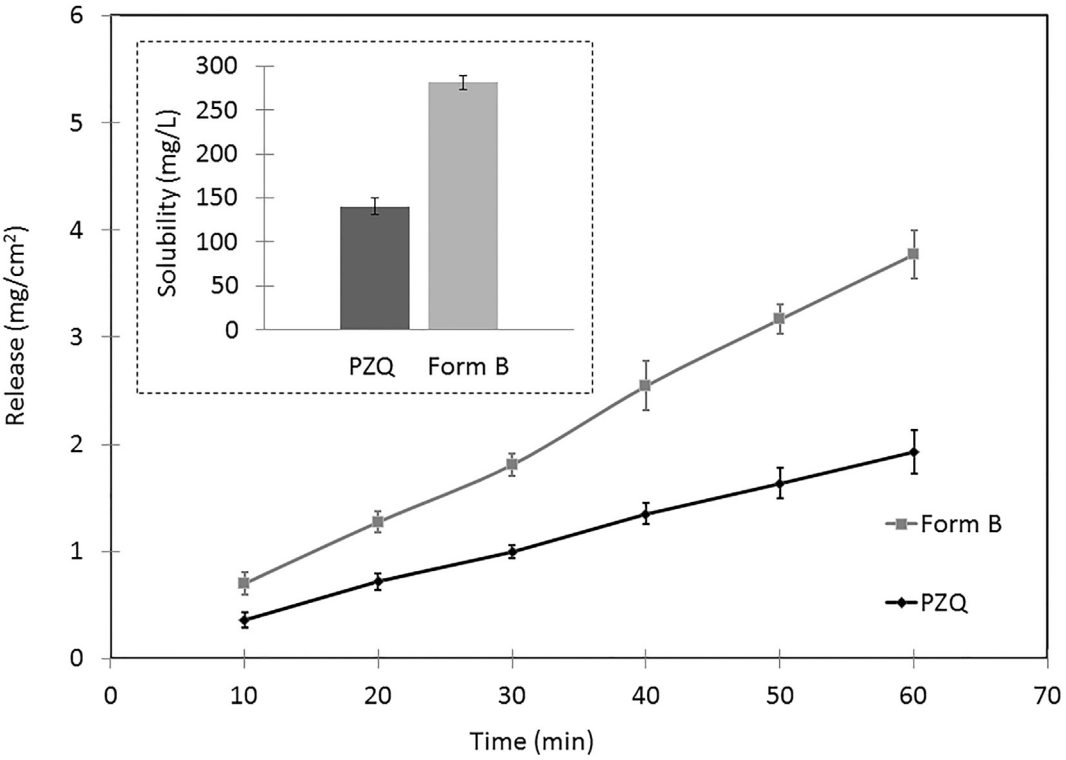

Fig. 11. Solubility and intrinsic dissolution of PZQ and Form B.

financed by the project Equip@Meso (ANR-10-EQPX-29-01) of the program «Investissements d'Avenir» supervised by the Agence Nationale de la Recherche.

References

[1] T. Nogi, J. Zhang, J.D. Chan, J.S. Marchant, A novel biological activity of praziquantel requiring voltage-operated Ca^{2+} channel b subunits: subversion of flatworm regenerative polarity, PLoS Negl. Trop. Dis. 3 (6) (2009) e464 1–13.

[2] WHO model list of essential medicines, 19 ed. (April 2015-Revised June 2015) Available at < http://www.who.int/selection_medicines/committees/expert/20/EML_2015_FINAL_amended_JUN2015.pdf?ua=1 > via the internet. WHO model list of essential medicines for children, 19 ed. (April 2015 - Revised June 2015) Available at: < http://www.who.int/selection_medicines/committees/expert/20/EMLc_2015_FINAL_amended_JUN2015.pdf?ua=1 via the internet > .

[3] M. Lindenberg, S. Kopp, J.B. Dressman, Classification of orally administered drugs on the World Health Organization Model list of essential medicines according to the biopharmaceutics classification system, Eur. J. Pharm. Biopharm. 58 (2) (2004) 265–278.

[4] J. Huang, S.P. Bathena, Y. Alnouti, Metabolite profiling of praziquantel and its analogs during the analysis of in vitro metabolic stability using information-dependent acquisition on a hybrid triple quadrupole linear ion trap mass spectrometer, Drug Metab. Pharmacokinet. 25 (5) (2010) 487–499.

[5] M. Talaat, F. Dewolfe Miller, A mass chemotherapy trial of praziquantel on Schistosoma haematobium endemicity in Upper Egypt, Am. J. Trop. Med. Hyg 59 (4) (1998) 546–550.

[6] P. de La Torre, S. Torrado, S. Torrado, Preparation, dissolution and characterization of praziquantel solid dispersions, Chem. Pharm. Bull. 47 (11) (1999) 1629–1633.

[7] S.K. El-Arini, H. Leuenberger, Dissolution properties of praziquantel–PVP systems, Pharm. Acta Helv. 73 (2) (1998) 89–94.

[8] E.D. Costa, J. Priotti, S. Orlandi, D. Leonardi, M.C. Lamas, T.G. Nunes, H.P. Diogo, C.J. Salomon, M.J. Ferreira, Unexpected solvent impact in the crystallinity of praziquantel/poly(vinylpyrrolidone) formulations. A solubility, DSC and solid-state NMR study, Int. J. Pharm. 511 (2) (2016) 983–993.

[9] M.V. Chaud, A.C. Lima, M.M.D.C. Vila, M.O. Paganelli, F.C. Paula, L.N. Pedreiro, M.P.D. Gremiao, Development and evaluation of praziquantel solid dispersions in sodium starch glycolate, Trop. J. Pharm. Res. 12 (2013) 163–168.

[10] G. Becket, L.J. Schep, M.Y. Tan, Improvement of the in vitro dissolution of praziquantel by complexation with α-, β- and γ-cyclodextrins, Int. J. Pharm. 179 (1999) 65–71.

[11] S. Maragos, H. Archontaki, P. Macheras, G. Valsami, Effect of cyclodextrin complexation on the aqueous solubility and solubility/dose ratio of praziquantel, AAPS PharmSciTech 10 (4) (2009) 1444.

[12] L. Yang, Y. Geng, H. Li, Y. Zhang, J. You, Y. Chang, Enhancement the oral bioavailability of praziquantel by incorporation into solid lipid nanoparticles, Pharmazie 64 (2) (2009) 86–89.

[13] B. Perissutti, N. Passerini, R. Trastullo, J. Keiser, D. Zanolla, G. Zingone, D. Voinovich, B. Albertini, An explorative analysis of process and variables affecting comilling in a vibrational mill: the case of Praziquantel, Int. J. Pharm. 533 (2) (2017) 402–412.

[14] R. Trastullo, L.S. Dolci, N. Passerini, B. Albertini, Development of flexible and dispersible oral formulations containing praziquantel for potential schistosomiasis treatment of pre-school age children, Int. J. Pharm. 495 (1) (2015) 536–550.

[15] N. Passerini, B. Albertini, B. Perissutti, L. Rodriguez, Evaluation of melt granulation and ultrasonic spray congealing as techniques to enhance the dissolution of praziquantel, Int. J. Pharm. 318 (1–2) (2006) 92–102.

[16] J. Bernstein, Polymorphism in Molecular Crystals. Polymorphism in Molecular Crystals, Clarendon Press, Oxford, 2002.

[17] D. Giron, Thermal analysis and calorimetric methods in the characterisation of polymorphs and solvates, Thermochim. Acta 248 (1995) 1–59.

[18] J. Bauer, S. Spanton, R. Henry, J. Quick, W. Dziki, W. Porter, J. Morris, Ritonavir: an extraordinary example of conformational polymorphism, J. Pharm. Res. 18 (2001) 859–866.

[19] J.C. Espinosa-Lara, D. Guzman-Villanueva, J.I. Arenas-García, D. Herrera-Ruiz, J. Rivera-Islas, P. Román-Bravo, H. Morales-Rojas, H. Höpfl, Cocrystals of active pharmaceutical ingredients praziquantel in combination with oxalic, malonic, succinic, maleic, fumaric, glutaric, adipic and pimelic acids, Cryst. Growth Des. 13 (2013) 169–185.

[20] T. Meyer, H. Sekljic, S. Fuchs, H. Bothe, D. Schollmeyer, C. Miculka, A New incentive to switch to (R)-praziquantel in schistosomiasis treatment, PLoS Negl. Trop. Dis. 3 (1) (2009) e357 1–5.

[21] A. Borrego-Sánchez, C. Viseras, C. Aguzzi, C.I. Sainz-Díaz, Molecular and crystal structure of praziquantel. Spectroscopic properties and crystal polymorphism, Eur. J. Pharm. Sci. 92 (2016) 266–275.

[22] O. Sanchez-Guadarrama, F. Mendoza-Navarro, A. Cedillo-Cruz, H. Jung-Cook, J.I. Arenas-Garcia, A. Delgado-Diaz, D. Herrara-Ruiz, H. Morales-Rojas, H. Hopfl, Chiral resolution of RS-praziquantel via diastereomeric Co-Crystal pair formation with malic acid, Cryst. Growth Des. 16 (1) (2015) 307–314.

[23] R. Toro, J. Kaduk, M. Delgado, G. Díaz de Delgado, Structural characterization of praziquantel: a broad spectrum anthelmintic, in powder diffraction. Powder Diffr. 2014, in: Proceedings of the International Centre for Diffraction Data (ICDD) Annual Spring Meetings, vol. 29, issue no 2, 2014, pp. 206–207.

[24] Y. Sun, S.J. Bu, Simple, cheap and effective high-performance liquid chromatographic method for determination of praziquantel in bovine muscle, J. Chromatogr. B 899 (2012) 160–162.

[25] A. Cedillo-Cruz, M.I. Aguilar, M. Flores-Alamo, F. Palomares-Alonso, H. Jung-Cook, A straightforward and efficient synthesis of praziquantel enantiomers and their 40-hydroxy derivatives, Tetrahedr.: Asymm. 25 (2) (2014) 133–140.
[26] P. Roszkowski, J.K. Maurin, Z. Czarnocki, Enantioselective synthesis of (R)-(−)-praziquantel (PZQ), Tetrahed.: Asymm. 17 (9) (2006) 1415–1419.
[27] A. Lausi, M. Polentarutti, S. Onesti, J.R. Plaisier, E. Busetto, G. Bais, L. Barba, A. Cassetta, G. Campi, D. Lamba, A. Pifferi, S.C. Mande, D.D. Sarma, S.M. Sharma, G. Paolucci, Status of the crystallography beamlines at Elettra, EPJ Plus 130 (3) (2015) 1–8.
[28] A.P. Hammersley, S.O. Svensson, M. Hanfland, A.N. Fitch, D. Häusermann, Two-q dimensional detector software: from real detector to idealised image or two-theta scan. High Press. Res. 14 (1996) 235–248. Hammersley, A. P. ESRF Internal Report 1998, ESRF98HA01T, FIT2D V9.129 Reference Manual V3.1.
[29] S.J. Clark, M.D. Segall, C.J. Pickard, P.J. Hasnip, M.J. Probert, K. Refson, M.C. Payne, First principles methods using CASTEP, Z. Kristallogr. – Cryst. Mater. 220 (2005) 567–570.
[30] P.J. Hasnip, K. Refson, M.I.J. Probert, J.R. Yates, S.J. Clark, C.J. Pickard, Density functional theory in the solid state, Philos. Trans. R. Soc. A-Math. Phys. Eng. Sci. 372 (2014) 20130270.
[31] C.J. Pickard, F. Mauri, All-electron magnetic response with pseudopotentials: NMR chemical shifts, Phys. Rev. B. 63 (2001) 245101.
[32] J.P. Perdew, K. Burke, M. Ernzerhof, Generalized gradient approximation made simple, Phys. Rev. Lett. 77 (1996) 3865–3868.
[33] E.R. McNellis, J. Meyer, K. Reuter, Azobenzene at coinage metal surfaces: role of dispersive van der Waals interactions, Phys. Rev. B. 80 (2009) 205414.
[34] A. Tkatchenko, M. Scheffler, Accurate molecular Van Der Waals interactions from ground-state electron density and free-atom reference data, Phys. Rev. Lett. 102 (2009) 73005.
[35] M.I. Suleiman, E.I.A. Karim, K.E.E. Ibrahim, B.M. Ahme, A.E.M. Saeed, A.E.M.E. Hamid, Photothermal stability of praziquantel, Saudi Pharmaceut. J. 12 (4) (2004) 157–162.
[36] I. Meister, K. Ingram-Sieber, N. Cowan, M. Todd, M.N. Robertson, M. Meli, M. Patra, G. Gasser, J. Keiser, Activity of praziquantel enantiomers and main metabolites against schistosoma mansoni, Antimicrob. Agents Chemother. 58 (9) (2014) 5466–5472.
[37] S.H. Xiao, J. Keiser, J. Chollet, J. Utzinger, Y. Dong, Y. Endriss, J.L. Vennerstrom, M. Tanner, In vitro and in vivo activities of synthetic trioxolanes against major human schistosome species, Antimicrob. Agents Chemother. 51 (4) (2007) 1440–1445.
[38] Y. Liu, X. Wang, J.K. Wang, C.B. Ching, Structural characterization and enantioseparation of the chiral compound praziquantel, J. Pharm. Sci. 93 (12) (2004) 3039–3046.
[39] S.K. El-Arini, D. Giron, H. Leuenberger, Solubility properties of racemic Praziquantel and its enantiomers, Pharm. Dev. Technol. 3 (4) (1998) 557–564.
[40] H.I. El-Subbagh, A.A. Al-Badr, Praziquantel, in: K. Florey (Ed.), Analytical Profile of Drug Substances and Excipients, Academic Press, New York, 1998, pp. 463–500.
[41] A. Altomare, C. Cuocci, C. Giacovazzo, A. Moliterni, R. Rizzi, N. Corriero, A. Falcicchio, EXPO2014, J. Appl. Cryst. 46 (2013) 1231–1235.
[42] A.A. Coelho, TOPAS-Academic, version 4.1, Coelho Software, Brisbane, Australia, 2007.
[43] Y. Liu, X. Wang, J.-K. Wang, C.B. Ching, Investigation of the phase diagrams of chiral praziquantel, Chirality 18 (2006) 259–264.
[44] A. Spek, Structure validation in chemical crystallography, Acta Cryst. D65 (2) (2009) 148–155.
[45] M. Baldrighi, D. Bartesaghi, G. Cavallo, M.R. Chierotti, R. Gobetto, P. Metrangolo, T. Pilati, G. Resnati, G. Terraneo, Polymorphs and co-crystals of haloprogin: an antifungal agent, CrystEngComm 16 (2014) 5897–5904.
[46] R.K. Harris, Applications of solid-state NMR to pharmaceutical polymorphism and related matters, J. Pharm. Pharmacol. 59 (2007) 225–239.
[47] D. Braga, L. Maini, C. Fagnano, P. Taddei, M.R. Chierotti, R. Gobetto, Polymorphism in crystalline cinchomeronic acid, Chem.-Eur. J. 13 (2007) 1222–1230.
[48] S.D. Gumbert, M. Korbitzer, E. Alig, M.U. Schmidt, M.R. Chierotti, R. Gobetto, X. van de Li, J. Streek, Crystal structure and tautomerism of Pigment Yellow 138 determined by X-ray powder diffraction and solid-state NMR, Dyes Pigments 131 (2016) 364–372.
[49] E. Salager, G.M. Day, R.S. Stein, C.J. Pickard, B. Elena, L. Emsley, Powder crystallography by combined crystal structure prediction and high-resolution 1H solid-state NMR spectroscopy, J. Am. Chem. Soc. 132 (2010) 2564–2566.
[50] A. Borrego-Sánchez, A. Hernández-Laguna, C.I. Sainz-Díaz, Molecular Modeling and Infrared and Raman spectroscopy of the crystal structure of the antiparasitic drug Praziquantel, J. Mol. Model. 23 (4) (2017) 106.
[51] D. Hasa, D. Voinovich, B. Perissutti, G. Grassi, S. Fiorentino, R. Farra, M. Abrami, I. Colombo, M. Grassi, Reduction of melting temperature and enthalpy of drug crystals: theoretical aspects, Eur. J. Pharm. Sci. 50 (1) (2013) 17–28.